Automated Design of an air/fuel controller for an SI engine considering the three-way catalytic converter in the H_∞ approach

C. A. Roduner, C. H. Onder, H. P. Geering
Department of Mechanical Engineering
Swiss Federal Institute of Technology (ETH) Zurich, Switzerland
roduner@imrt.mavt.ethz.ch

Abstract

The correct operation of the emissions reduction system of an SI engine depends on the capability of the three-way catalyst (TWC) to store and release oxygen. Either one or the other is lost if the oxygen storage of the TWC is completely full or completely empty. In order to optimally handle upstream air-to-fuel ratio (lambda) excursions in either direction (lean or rich), the stored oxygen mass should be kept near the middle of the current oxygen storage capacity.

An H_∞ controller is developed which takes into account the dynamic behavior of the TWC. The main design goal is to compensate the disturbance impact on the relative oxygen storage level by first measuring the upstream air-to-fuel ratio only. For this purpose the TWC is regarded as a limited integrator. The dynamics of the fuel-path subsystem of the engine (between fuel injection and measured upstream air-to-fuel ratio) is modeled by a lowpass element and a time delay connected in series. Since the engine parameters vary with each operating point, a gain-scheduled controller is used to achieve optimal performance in the entire operating range. To recognize errors in observation of the relative oxygen storage level due to an offset of the upstream lambda sensor, a second sensor behind the TWC is needed. A slower PI controller is superimposed on the H_∞ control system to compensate these observation errors.

Measurements on an engine test bench illustrate the performance of the control system.

1 Introduction

The air-to-fuel ratio control is one of the most important control loops in engine control since the TWC is able to show its best emissions reducing ability only if the engine is run at stoichiometry. Due to the ability of the TWC to store oxygen and carbon monoxide on its surface, short excursions of the air/fuel ratio can be managed as long as they do not exceed the remaining storage capacity. Therefore it is of interest to keep the storage level of the TWC always in its middle.

Conventional lambda controllers use switch type oxygen sensors. These sensors give only very limited information on the size of the lambda excursion. Therefore, a storage level control (buffer control) can be implemented only with strong limitations. Other drawbacks of the switch type sensor are the resulting limit cycle of the control system and the very heuristic control design methodology (i.e., the „step-ramp" parameters of the controller have to be found by trial and error experiments).

With the new UEGO (universal exhaust gas oxygen) sensors a new type of air-to-fuel ratio controller is now possible. Since the sensor has linear dynamics a linear model-based control design is possible. The size of the lambda excursion is now known. Therefore the total amount of excess or missing oxygen which has to be stored in the catalytic converter can now be calculated and taken into account as well.

2 Plant

The plant to be controlled is the fuel path of an SI engine up to the catalytic converter. It is depicted in Fig. 1.

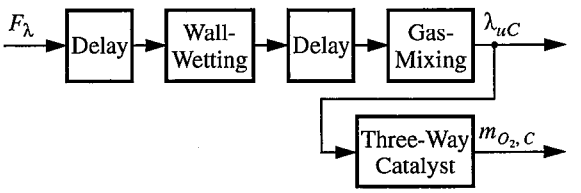

Figure 1: Flowchart of the fuel path

The input F_λ of the plant is a multiplicative factor for the injection duration. The outputs are the lambda value at the main confluence point λ_{uC} (upstream of the TWC) and the mass of oxygen stored in the TWC $m_{O_2,C}$. The system up to the main confluence point has already been investigated in detail [1]. For control purposes, that model is much too complicated. Therefore the complete air-to-fuel ratio path from the fuel injectors up to the UEGO sensor at the main confluence point is approxi-

mated by a series connection of a first order lag and a delay (Eq. 1):

$$G(s) = \frac{\Delta\lambda_{uC}}{\Delta F_\lambda} = \frac{-1}{s\tau + 1} e^{-sT} \tag{1}$$

The parameters of this model, i.e., the time constant τ of the lag element and the time delay T, are dependent on the operating point of the engine defined by the engine speed n and the mass of air in one cylinder $m_{air,cyl.}$. An identification for these two parameters has been presented earlier [2]. Therefore a complete map of these two parameters can easily be obtained.

In order to apply an H_∞ control design a linear, finite dimensional system is required. Thus, the time delay is approximated with a Padé allpass element (Eq. 2). This has been found to be the best approximation method in this context. The order n_{apx} of the approximation is chosen as a function of the size of the time delay. For delays up to 40 ms a first order approximation is chosen, and for every additional 40 ms, one order is added. This results in a conservative approximation of the delay. However, this is no drawback due to the order reduction following the control design.

$$e^{-sT} \cong \frac{\sum_{j=0}^{n_{apx}} a_j(-sT)^j}{\sum_{j=0}^{n_{apx}} a_j(sT)^j} \qquad a_j = \frac{(2n_{apx}-j)!\,n_{apx}!}{j!(n_{apx}-j)!\,2n_{apx}!} \tag{2}$$

Since the three way catalytic converter (TWC) is capable of storing oxygen (O_2) as well as carbon monoxide (CO), it is not the actual value of the air-to-fuel ratio that is relevant for the tailpipe (downstream of the TWC) emissions. As long as excess or missing oxygen can still be stored in the TWC, no higher emissions are expected downstream of the TWC. (Missing oxygen describes rich gas mixtures which result in CO.) Only if the storage of the TWC is full or depleted, a rise in NO or CO and HC concentration, respectively, is expected. Therefore an integrator is added to the dynamics described above to model the storage behavior of the TWC:

$$\Delta m_{O_2,C} = \frac{1}{s} \cdot \overset{*}{m}_{O_2,uC} \cdot \Delta\lambda_{uC} \tag{3}$$

$\overset{*}{m}_{O_2,uC}$ defines the oxygen mass flow at the upstream UEGO sensor. For the linear control design we assume that $\overset{*}{m}_{O_2,uC} = 1$. In the controller realization the correct mass flow will be considered.

3 Control Design

The goal of the controller is to minimize the disturbance impact of a lambda deviation on the oxygen storage level of the TWC by measuring only the upstream lambda with a UEGO sensor (see Fig. 2). The transfer

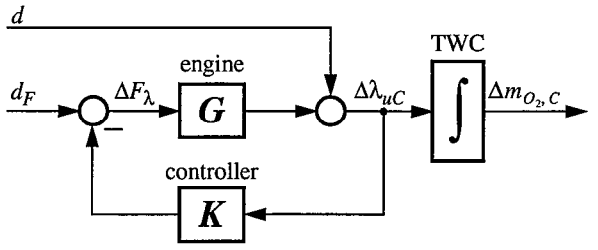

Figure 2: Flowchart of the upstream lambda control system

function from the disturbance d to the stored oxygen mass $\Delta m_{O_2,C}$ is given in Eq. 4:

$$G_{Cd}(s) = \frac{\Delta m_{O_2,C}}{d} = \frac{1}{s}(1 + G(s)K(s))^{-1} \tag{4}$$

For the design of an H_∞ controller we have to extend the control scheme with weighting functions (see Fig. 3).

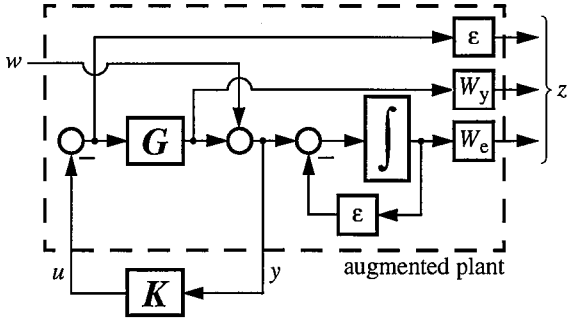

Figure 3: Extended control system of the H_∞ problem

The two ε are very small and are introduced only to guarantee the numerical solvability of the H_∞ problem. The transfer matrix of the closed loop system T_{zw} for $\varepsilon = 0$ is shown in Eq. 5:

$$T_{zw} = \begin{bmatrix} W_e \cdot G_{Cd} \\ W_y \cdot T_e \end{bmatrix} \qquad T_e = GK(1+GK)^{-1} \tag{5}$$

For $\gamma = 1$, Eq. 6 follows:

$$\begin{aligned} |G_{Cd}(j\omega)| &< |W_e^{-1}(j\omega)| \\ |T_e(j\omega)| &< |W_y^{-1}(j\omega)| \end{aligned} \qquad \forall\omega \tag{6}$$

The dynamic weight W_e serves thus for defining an upper bound for the magnitude of the disturbance transfer function G_{Cd}. W_e is chosen according to Eq. 7:

$$W_e(s) = \frac{1}{d_{max}} \cdot \frac{s + \omega_c}{s + \varepsilon} \tag{7}$$

The influence of the two design parameters d_{max} and ω_c can be seen in Fig. 4. The value d_{max} defines a horizontal

limit for the magnitude of G_{Cd} and therefore limits its maximal value. At low frequencies the behavior is forced to be integrating to avoid steady state errors (for numerical reasons the pole is not exactly at 0). This results in a left boundary for the magnitude of G_{Cd}. With ω_c this boundary can be moved horizontally.

To avoid an unnecessarily high bandwidth of the control system, the complementary sensitivity T_e is limited with an appropriate choice of W_y:

$$W_y(s) = \frac{s}{13 \cdot \omega_c} \tag{8}$$

These two weighting functions are illustrated in Figs. 4 and 5.

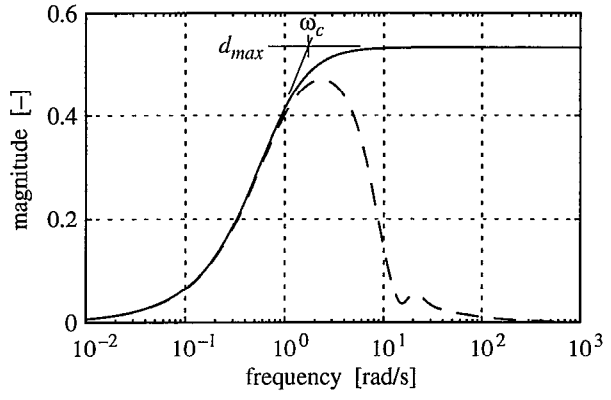

Figure 4: Magnitude of W_e^{-1} (solid) and G_{Cd} (dashed)

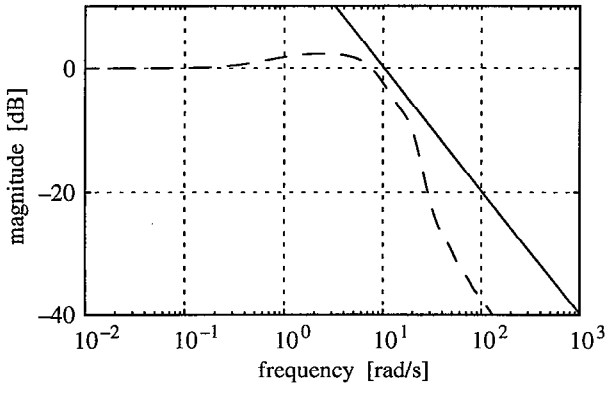

Figure 5: Magnitude of W_y^{-1} (solid) and T_e (dashed)

The plant parameters T and τ vary over quite a large range. For the BMW M42 engine the following range can be assumed:

$$T \in [0.02, 1.0]\ \text{s}, \qquad \tau \in [0.01, 0.5]\ \text{s/rad}$$

Since the time delay can not be compensated, the performance demands have to be adjusted for varying operating points. For large time delays it is therefore mandatory that the demanded bandwidth of the control system is reduced. The time constant can always be perfectly compensated and therefore has no influence on the weighting functions. This leads to the following empirically found design parameters:

$$d_{max} = f_{d_{max}} \cdot T, \qquad \omega_c = \frac{f_{\omega_c}}{T} \tag{9}$$

This choice of the design parameters results in an almost identical Nyquist diagram for G_{Cd} and thus in the same robustness over the whole operating range. The parameters $f_{d_{max}}$ and f_{ω_c} allow a certain shaping of the Nyquist diagram. The following values have been found to be adequate:

$$f_{d_{max}} = 1.9, \qquad f_{\omega_c} = 0.22$$

Since the phase shift of the time delay can not be avoided, a robust stabilizing controller has to place significant actuator energy (i.e., high gain) at the opposite of the Nyquist point. This results in one or several characteristic „bubbles" in the right halfplane (see Fig. 6). This high gain at frequencies higher than the crossover frequency results in a differential behavior which adds damping to the control system if the modeling error of the time delay is small. An error in the identified time delay results in an additional rotation of the Nyquist curve. Thus, using more than one bubble increases the demand of very accurate modeling and is therefore omitted. This behavior (one bubble) can always be realized with a 4th order controller (the bubble requires a complex conjugate pair of poles). If not even one bubble is necessary or wanted, then the minimal order of the controller becomes two (two poles at zero which avoid a steady state error in $\Delta m_{O_2,C}$).

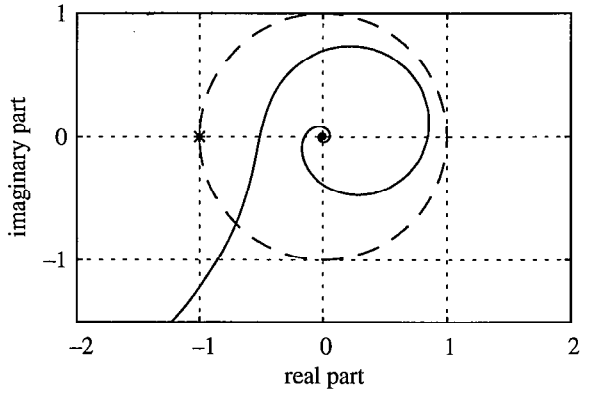

Figure 6: Nyquist plot of the control loop

For a 10 % step in the disturbance d, the control design results in the step response depicted in Fig. 7. In the plot the influence of d_{max} and ω_c on the traces is shown with arrows. Diminishing d_{max} results primarily in a faster descent of lambda back to stoichiometric and thus in a

smaller peak of the be stored oxygen amount. Enlarging ω_c then results in a faster descent of the total oxygen. The return of the stored oxygen mass to its nominal value can obviously only be achieved if $\Delta\lambda_{uC}$ does not return directly to zero but overshoots to obtain areas above and below the abscissa of equal sizes (with constant air mass flow assumed).

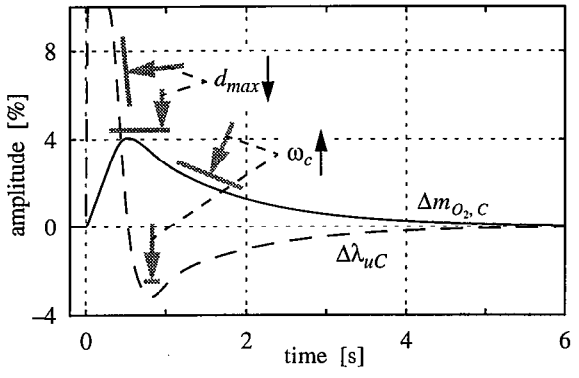

Figure 7: Response of the control system for a 10 % step in the disturbance d

The results in Figs. 4 – 7 are simulated for a time constant of 0.192 s and a time delay of 0. 276 s.

4 Realization of the controller

Due to the Padé approximation of the delay, the order of the controller rises with increasing delay. However, as discussed above, a fourth order controller is sufficient. Therefore the variable order of the controller after the design procedure is reduced without any loss in accuracy. The order reduction is done with a minimal change in G_{Cd} which can be achieved with a dynamic weighting of the compensator prior to the balancing [4], [5].

The fourth order controller can be realized with several state-space descriptions. Due to the order reduction, the states of the controller for each operating point are different and allow no physical interpretation. Since the designed controller has to be gain-scheduled a fixed, physically motivated structure has to be found. This structure has to incorporate the minimum number of parameters (seven: a general fourth order controller has nine parameters, in our case two poles are forced to zero) and must minimize the sensitivity to parameter errors which is achieved by paralyzing the structure as much as possible. This leads to the following controller transfer function:

$$K(s) = G_1 + G_2\frac{1}{s} + G_3\frac{1}{s^2} + G_4\frac{s(G_7 s+1)}{G_5^2 s^2 + 2G_6G_5 s + 1} \quad (10)$$

$G_1 - G_7$ are functions of the time delay and the time constant, or directly of the operating point defined by engine speed and load.

For a realistic physical model of the storage behavior the varying mass flow through the TWC has to be taken into account. This is done by multiplying the lambda deviation $\Delta\lambda_{uC}$ with the air mass flow $\overset{*}{m}_{O_2,uC}$ before it is integrated. Afterwards, it is divided again, as depicted in Fig. 8. Thus a physical oxygen balance is obtained without changing the input-output behavior at a fixed operating point. The limits of the oxygen storage of the TWC (zero, $C_{O_2,C}$) have to be modeled as well.

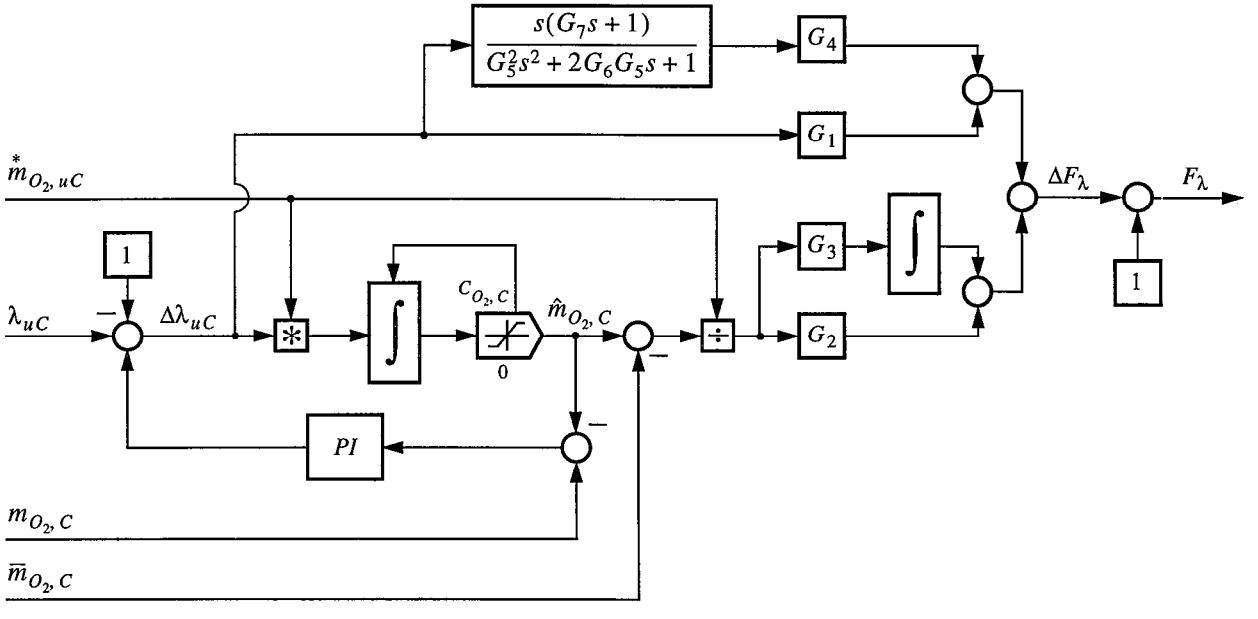

Figure 8: Complete controller

Due to different raw gas composition in every operating point, the UEGO sensor has a varying offset. This offset and an error in the observed amount of oxygen has to be corrected with an overlying control loop. A very slow PI controller can be chosen, for example. A sensor signal from downstream of the TWC has to be interpreted as the oxygen level. The difference between this measured oxygen level $m_{O_2,C}$ and the observed level $\hat{m}_{O_2,C}$ is the input of the PI controller. The feedback controller of the upstream lambda sensor works as a feed-forward controller for the control of the TWC.

The gain G_3 is placed in front of the second (right) integrator to avoid an excitation of the controller due to varying operating points.

5 Experimental results

The experiments were performed on a 1.8 l BMW 4 cylinder engine. At the main confluence point a BOSCH UEGO sensor (LSU4) is used for the air-to-fuel ratio measurement. The controller was implemented on an engine management system written in PASCAL running on a hp1000 process controller in an event-based mode. The synchronization of the spark and fuel injection actuators with the engine is achieved with a VLSI chip built at ETH [3].

To demonstrate the varying bandwidth of the control system, two operating points are shown (see Table 1).

Table 1: Operating points chosen

Operating point	OP 1	OP 2
Engine speed n [rpm]	1500	1500
Mass air in cylinder $m_{air,cyl.}$ [g]	0.1	0.3
Engine torque [Nm]	18	80
Time delay T [s]	0.276	0.116
Time constant τ [s]	0.192	0.146
Segment time [s]	0.02	0.02
Cycle time [s]	0.08	0.08

Note that the first operating point (OP 1) was used for the simulations in Section 3. The time delay and the time constant of the plant are identified according to [2] with a colored noise as excitation. At OP 1 the time delay corresponds to nearly 14 segments (samples) which is 7 engine revolutions for a 4 cylinder engine.

Fig. 9 shoes a comparison between measured step responses at OP 1 and a simulation with the corresponding values in Table 1 (the identification was not done with these measurements). The step from rich to lean as well as the step from lean to rich are made at 0 s. Obviously

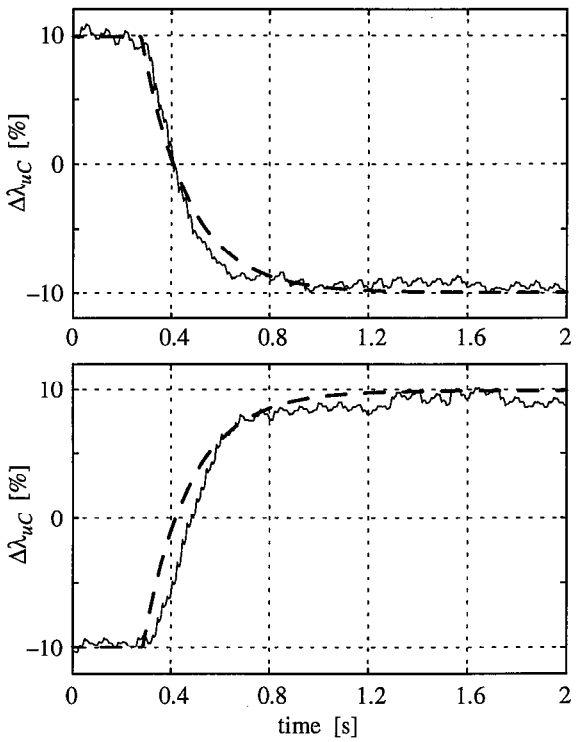

Figure 9: Simulated (dashed) and measured step response of the plant at OP 1

the plant is fitted very well. A certain asymmetric behavior can be recognized. This can of course not be matched with the linear model. As opposed to the results of measurements with switch type sensors, no step behavior at the stoichiometric point is present. Thus the sensor itself has very linear dynamics. The ripple in the measurement results are the cylinder-to-cylinder deviations. Thus the engine cycle time of 80 ms can clearly be seen.

Fig. 10 depicts the response of the upstream lambda buffer control system for a disturbance step at d_F of 20 % (see Fig. 2). The location d_F represents the more realistic input for a disturbance than location d. The latter represents the worst case because the disturbance acts immediately on the compensator and is therefore preferable for the control design. Again the agreement between measurement and simulation results is very good. The asymmetric behavior of the plant (as seen in Fig. 9) is now responsible for an asymmetric behavior of the control system. The measured overshoot due to a step in the rich direction of the disturbance is larger than the simulated one. Vice versa, the step in the lean direction results in a smaller measured overshoot.

Due to the time delays at OP 1 and OP 2 being different, the bandwidths of the control systems vary accordingly. The maximum deviation of the air-to-fuel ratio at OP 1 is larger because due to the larger time delay the controller is not able to react as soon as at OP 2. Also the

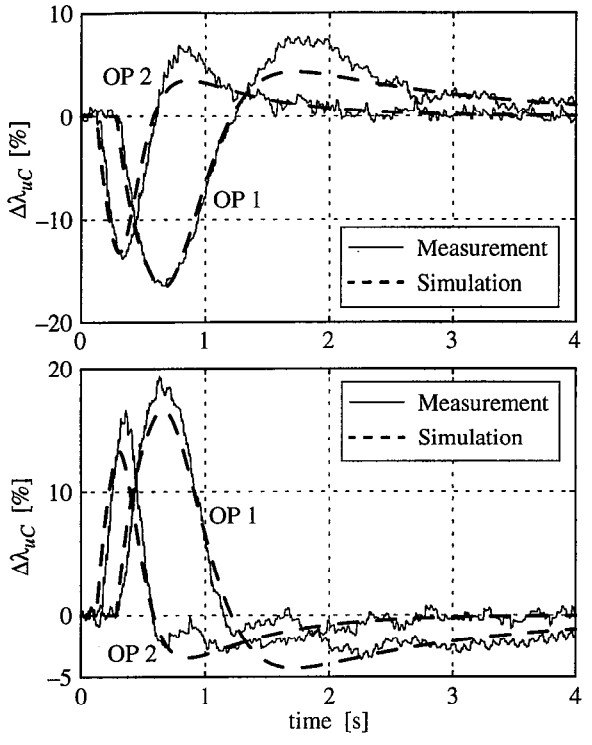

Figure 10: Response of the upstream lambda buffer control system to a 20 % step in d_F (see Fig. 2)

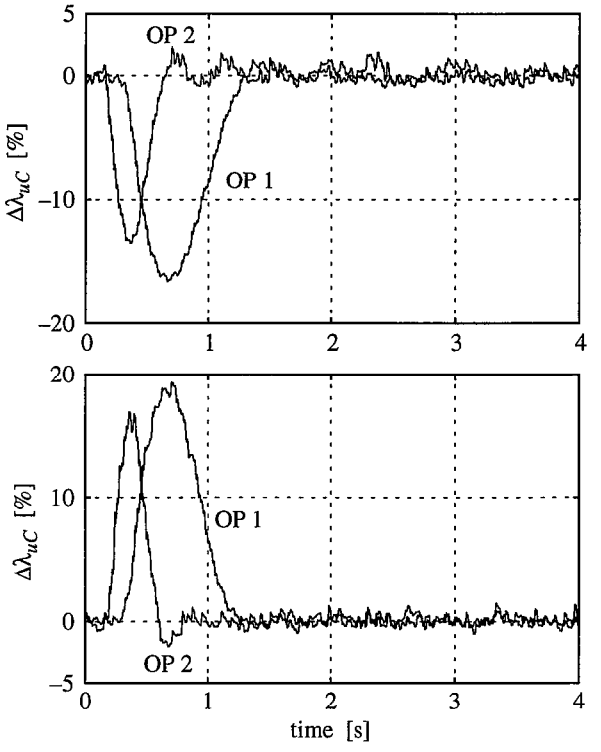

Figure 11: Response of the upstream lambda control system without buffer to a 20 % step in d_F (see Fig. 2)

maximum error in integrated lambda is much larger at OP 1 due to its smaller bandwidth. Nevertheless the error in stored oxygen is not higher due to the much smaller air mass flow.

To clearly show the difference between lambda and buffer control, measurement results at OP 1 and OP 2 with a lambda controller without buffer control are shown in Fig. 11. The compensating overshoot is no longer present. Therefore several disturbances in the same direction force the oxygen storage of the TWC to either its upper or lower limit, resulting in either NO or CO and HC emissions.

Fig. 12 shows the response of the complete control system to a throttle step. The throttle step was chosen to change from OP 1 to OP 2. Since the injected amount of fuel was calibrated only as a static function of the air mass flow into the manifold, a large λ_{uC} transient occurs. The first small transient in the lean direction is caused by the timing error. The second excursion (rich) is due to the manifold dynamics, while the third results from the wall-wetting dynamics. Although these deviations are up to 35 %, the controller manages to keep the voltage of the switch type sensor downstream of the TWC $U_{\lambda_{2PdC}}$ to remain between 560 mV and 580 mV. These voltages lie within the very sensitive region of stoichiometry of the sensor and indicate a very good conversion efficiency of the TWC.

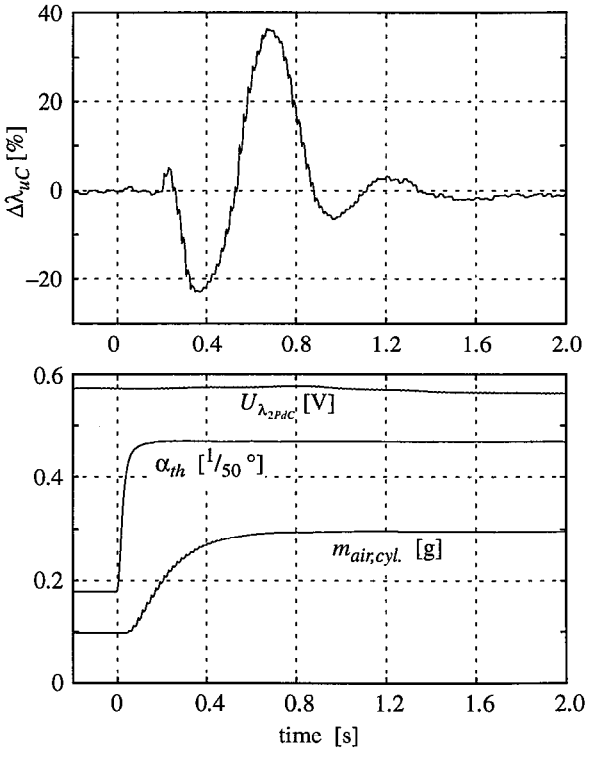

Figure 12: Response of the complete control system with buffer to a throttle step from OP 1 to OP 2

6 Conclusions

A new air/fuel ratio control scheme has been presented. It uses an UEGO sensor upstream of the TWC and takes the oxygen storage behavior of the TWC into account. The main goal is to control the oxygen level of the TWC (buffer control).

For this control scheme a fully automated design procedure has been developed. With an on-line identification scheme the plant parameters can be identified very efficiently. This results in two maps for the complete operating range. The controller parameters are then calculated from the plant parameters using H_∞ techniques and varying dynamic weighting functions.

The complete design procedure has been tested on an engine test bench and was found to be very efficient.

7 Acknowledgments

The research described in this article was funded by the Robert Bosch GmbH. The authors wish to thank E. Schnaibel, Dr. F. Blischke, and Dr. R. Deibert of the Robert Bosch GmbH for the many valuable discussions.

8 Nomenclature

physical variables

α_{th}	throttle angle
F_λ	multiplicative factor for the injection duration
ΔF_λ	$= F_\lambda - 1$
λ_{uC}	lambda value upstream of the TWC
$\Delta\lambda_{uC}$	$= \lambda_{uC} - 1$
$m_{air,cyl.}$	mass of air in one cylinder
$m_{O_2,C}$	stored mass of oxygen in the TWC
$\bar{m}_{O_2,C}$	demanded value for $m_{O_2,C}$
$\Delta m_{O_2,C}$	$= m_{O_2,C} - \bar{m}_{O_2,C}$
$\hat{m}_{O_2,C}$	estimated value for $m_{O_2,C}$
$\overset{*}{m}_{O_2,uC}$	oxygen mass flow at the upstream sensor
n	engine speed
$U_{\lambda_{2PdC}}$	voltage of the switch type sensor downstream of the TWC
T	time delay of the plant (overall time delay of the fuel path)
τ	time constant of the plant (significant time constant of the fuel path)
$C_{O_2,C}$	oxygen mass storage capacity of the TWC

mathematical variables

d	worst case disturbance on the control system
d_F	additive disturbance on the control signal ΔF_λ
u, w, y, z	input and output signals of the augmented plant of the H_∞ setup
G	plant of the control loop
G_{Cd}	plant of the performance index
K	controller
T_e	complementary sensitivity of the control system
T_{zw}	closed loop system of the H_∞ setup
W_e, W_y	weighting functions of the H_∞ setup
$G_1 - G_7$	(gain scheduled) parameters of the controller
ω_c, d_{max}	parameters of the weighting functions
f_{ω_c}, $f_{d_{max}}$	parameters of the control design
n_{apx}	order of the time delay approximation
s	complex variable
ω	frequency

9 References

[1] C. H. Onder, C. A. Roduner, H. P. Geering: „Model Identification for the A/F Ratio Path of an SI Engine." *SAE International Congress, SAE paper* 970612 *(included in SAE special publication* SP-1236, *Electronic Engine Control)*, Detroit, 1997.

[2] E. Shafai, C. A. Roduner, H. P. Geering: „On-Line Identification of Time Delay in the Fuel Path of an SI Engine." *SAE International Congress, SAE paper* 970613 *(included in SAE special publication* SP-1236, *Electronic Engine Control)*, Detroit, 1997.

[3] H. P. Geering: „ICX, a Custom VLSI-chip for Engine Control." *Int. J. of Vehicle Design*, vol. 10, pp. 592-597, 1989. (Also in: *Proceedings of the 5th IAVD Congress*, Geneva, pp. 465-471, 1989.)

[4] B. D. O. Anderson, Y. Liu: „Controller Reduction: Concepts and Approaches." *IEEE Trans. Automat. Contr.*, vol. 34, pp. 801-812, 1989.

[5] C. A. Roduner: *H_∞-Regelung linearer Systeme mit Totzeiten*. Diss. ETH, Swiss Federal Institute of Technology, Zurich, to appear in 1997.